Charge-Induced Modulation of Magnetic Interactions in a [2 × 2] Metal-organic Grid Complex

C. ROMEIKE,[1] M. R. WEGEWIJS,[1] W. WENZEL,[2] M. RUBEN,[2] H. SCHOELLER[1]

[1]*Institut für Theoretische Physik A, RWTH Aachen, Aachen, Germany*
[2]*Institut für Nanotechnologie, Forschungszentrum Karlsruhe, Postfach 3640, 76021 Karlsruhe, Germany*

ABSTRACT: We investigate the magnetic state of a recently synthesized [2 × 2]-metal-organic grid complex as a function of its redox state. Our analysis of a phenomenological model for the relevant molecular orbitals reveals that additional electrons on the ligands can couple their spins via the bridging metal sites. We find that at certain stages of the reduction of the complex cation, a maximal total spin ground state of the complex ($S = 3/2$) can be stabilized by the Nagaoka mechanism. © 2005 Wiley Periodicals, Inc. Int J Quantum Chem 106: 994–1000, 2006

Key words: molecular magnetism; spin crossover; magnetic interactions; macromolecular complex; metal-organic complex

Correspondence to: W. Wenzel; e-mail: wenzel@int.fzk.de
This article was presented at the Eighth European Workshop on Quantum Systems in Chemistry and Physics in Spetses, Greece, August 30 to September 4, 2003.
Contract grant sponsor: Deutsche Forschungsgemeinschaft.
Contract grant number: SCHO 641/3-1.
Contract grant sponsor: European Community.
Contract grant number: HPRN-CT-2002-00302.

1. Introduction

The synthesis and investigation of molecule-based magnets has been an active area of research for almost a decade [1, 2]. Today molecule-based magnets offer a wide variety of chemical and magnetic properties that have potential applications in a wide range of systems. Photomagnetic, e.g., $K_{0.4}Co_{1.3}[Fe(CN)_6]$, or spin-crossover magnetic substances, e.g., Fe(*o*-phenanthroline)$_2$(NCS)$_2$, offer potential applications in switchable devices. Interesting quantum tunneling effects were reported for Mn_{12} [3] and Fe_8 [4] clusters. Single molecular magnets (SMMs) bridge the gap between microscopic and macroscopic physics. For example, macroscopic quantum tunneling effects were observed in Mn_{12} [5], which may make these systems suitable for quantum computing applications [6].

Self-assembling metal–organic complexes offer one promising route to the design of spin-crossover complexes, in which intramolecular magnetic interactions can be modified through the choice of the metal and variation of the bridging ligand. One recently developed class of single molecular magnets are metal–organic complexes that self-assemble into [$M \times M$]-grid planar grid structures [7, 8]. The complex consists of M^2 metallic centers confined by two perpendicular arrays of rod-like ligands, each with M coordination sites. Several realizations of these supramolecules exhibit a variety of magnetic and electrochemical properties that are influenced by the side groups of the bridging ligands. In this investigation, we have analyzed the magnetic properties of the [2×2]-grid depicted in Figure 1, which consists of four organic ligands [bis(bipyridyl)bipyrimidine] and four Fe^{2+} transition-metal centers [9] as a prototypical example of this class of molecules. In solution, the cation is known to exhibit an impressive nine reduction steps in a cyclic voltammetry at $T = 253K$ [9]. It is also possible to trap complexes on a graphite surface in a controlled way [10, 11].

Spin coupling in SMM arises from a number of complex and partially competing interactions, which almost balance in spin-crossover compounds. Currently available ab initio techniques are often either too expensive to treat the large molecules involved or lack the energy resolution to treat all these interactions on the same footing. Present-day modeling can nevertheless act as a guide in the development of SMMs and spin-crossover compounds if it is possible to develop heuristic models for the relevant electronic degrees of freedom.

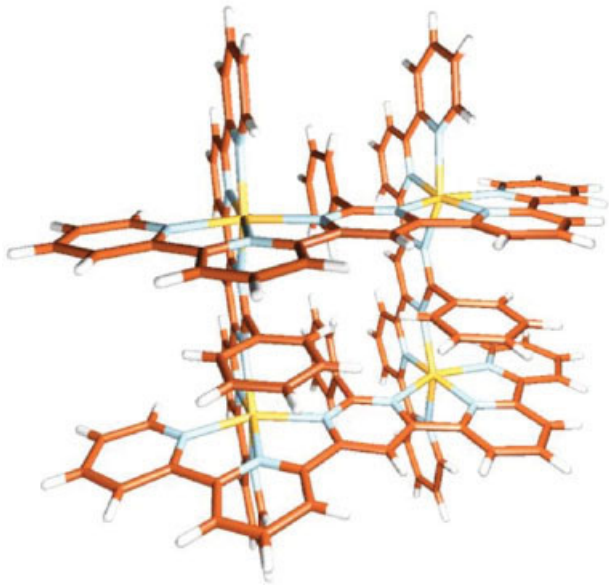

FIGURE 1. Structure of the [2×2]-grid-type complex.

We have developed a phenomenological model that represents the important spin and charge degrees of freedom that play a role in both the redox chemistry of the compound and its magnetic interactions. To study their interplay, we have analyzed this model by perturbative techniques. We find that additional electrons, which occupy orbitals on the ligands, are magnetically coupled via orbitals on the bridging metal ions. As expected, an antiferromagnetic order prevails in most regions of the parameter space. However, when the four ligand orbitals are near half-filling, a sufficiently strong Coulomb interaction can stabilize a maximal total spin ground state of the complex. Experimentally this effect may be realized chemically by introducing electron-donating side groups on the ligands [9].

This article is organized as follows. After a brief analysis of the electronic structure of the complex in Section 2.1, we introduce and motivate the phenomenological model for the metal–organic complex in Section 2.2. In Section 2.3, we discuss the perturbative treatment of the model, which provides a quantitative understanding of the cyclic voltammogram and predicts transition to maximal total spin $S = 3/2$ for sufficiently strong Coulomb charging on the ligand orbitals. The electron addition spectra and spin-coupling mechanism are pre-

sented in Section 3. In Section 4, we discuss the experimental implications of our analysis, in particular with respect to electron tunneling experiments.

2. Model

2.1. ELECTRONIC STRUCTURE

We have performed a number of exploratory in vacuo ab initio Hartree–Fock (HF) and density functional theory (DFT) calculations of the Fe^{2+} [2 × 2] grid complex. These calculations strain presently available computational resources and did not converge in all relevant charge sectors. Because of the large system size (>200 atoms) and the presence of transition metal ions, they lack the energetic resolution to differentiate among the spin states and cannot give reliable estimates of the ionization potentials and electron affinities required for the interpretation of the entire cyclic voltammogram. Nevertheless they guide the development of a quantitative phenomenological model based on the relevant electronic degrees of freedom.

The most important molecular orbitals (MOs) near the Fermi energy are either d-like orbitals on the metal ions or π-orbitals localized on the ligands. The four metal ions are situated in an approximately octahedral environment of nitrogen atoms (see Fig. 1). As predicted by ligand-field theory, a near-octahedral coordination of each metal ion causes their d-orbitals to split up into two shells: $t_{2g}(d_{xy}, d_{xz}, d_{yz})$ and $e_g(d_{x^2-y^2}, d_{z^2})$. A slight lowering of the symmetry to D_{2d} results in a small splitting of these shells. The total charge of 8+ of the complex is balanced by counterions. At low temperatures, each metal ion will be in its low-spin ground state. Low-spin Fe^{2+} has a completely filled t_{2g}-like shell, while the e_g-like orbitals are empty (see Fig. 2). We also note that the e_g orbitals have different approximate symmetry (σ) than that of energetically close ligand orbitals (π). As a result, it is sensible to distinguish between ligand and metal orbitals that hybridize only by weak tunnel coupling. Nevertheless, there are strong electrostatic interactions between electrons localized on the metal ions or on the ligands. The local Coulomb repulsion on the metal ions is larger than the on-site energy on the ligands because the metal orbitals are much more localized.

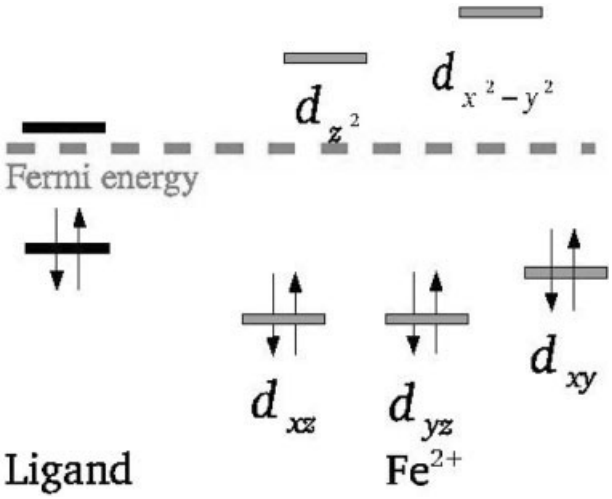

FIGURE 2. Orbital configuration of transition metal ions and ligands at Fermi energy. Note that $\Delta = \epsilon - E$ is negative.

2.2. PHENOMENOLOGICAL MODEL

These observations suggest the following phenomenological Hamiltonian for the electronic degrees of freedom of the complex: The [2 × 2]-grid complex is represented by four metal Fe^{2+} and four ligand sites, with one spin-degenerate orbital per site. There is a local Coulomb repulsion U/u for the metal ions/ligand orbitals, respectively, and long-range Coulomb interactions among the ligand orbitals on adjacent (v) and next-nearest (w) ligands ($w \ll v \ll u$). The orbital energy of the ligand/metal orbitals is denoted by ϵ/E, respectively. Finally, there is a weak hybridization between orbitals on metal ions and adjacent ligand orbitals. Figure 3 presents these interactions are schematically. The total Hamiltonian can thus be written as a sum of metal-ion and ligand terms, which are only weakly coupled:

$$H = H_L + H_M + H_T, \tag{1}$$

$$H_L = \sum_{i=1}^{4} [\epsilon(n_{i,\uparrow} + n_{i,\downarrow}) + u n_{i,\uparrow} n_{i,\downarrow} + v n_i n_{i+1}] + w \sum_{i=1}^{2} n_i n_{i+2} \tag{2}$$

$$H_M = \sum_{\sigma,i=1}^{4} E N_{i,\sigma} + U N_{i,\uparrow} N_{i,\downarrow} \tag{3}$$

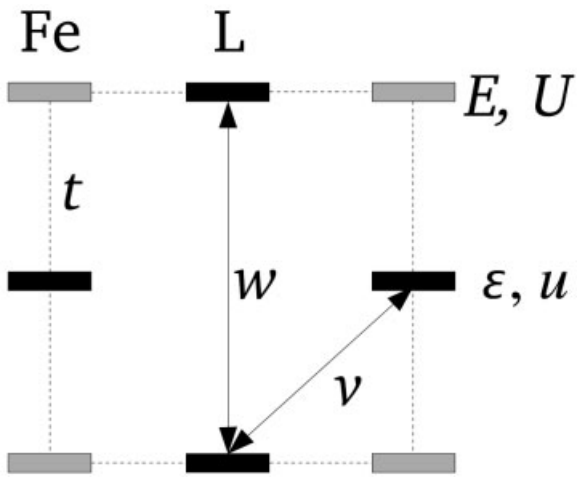

FIGURE 3. Geometry of transition metal [2 × 2] grid of Fe^{2+} metals with bridging ligands *L*. Hopping amplitudes *t*, orbital energies *E*, ϵ, and Coulomb charging energies *U*, *u*, *v*, *w* are shown schematically.

$$H_T = \sum_{\langle i,j\rangle} \sum_{\sigma} t A^{\dagger}_{i,\sigma} a_{j,\sigma} + h.c. \tag{4}$$

Operators and variables in lower/uppercase relate to the metal/ligands (except *t*). $\langle i, j\rangle$ denotes a summation over nearest-neighbor metals (i = 1–4) and ligands (j = 1–4). The Fermion operator $a^{\dagger}_{i,\sigma}(a_{i,\sigma})$ creates (destroys) an electron on ligand site i = 1–4 with spin projection $\sigma = \pm 1/2$. The occupation number operator is defined as usual $n_{i,\sigma} = a^{\dagger}_{i,\sigma} a_{i,\sigma}$ and $n_i = \sum_{\sigma} n_{i,\sigma}$. Similar definitions hold for the metal ($A_{j,\sigma}$, $N_{i,\sigma} = A^{\dagger}_{i,\sigma} A_{i,\sigma}$). The tunneling term (4) describes hopping between ligand and metal sites. Assuming a symmetric molecular structure, the hopping matrix elements *t* are identical for all sites.

Experimental results [9] suggest that the first eight additional electrons will occupy the ligand's lowest unoccupied molecular orbitals (LUMO). We must then assume that the Fe^{2+} orbital energy *E* lies above two charge states of the ligand: $\epsilon < \epsilon + u < E < E + U$. The orbital energy difference $\Delta = \epsilon - E < 0$ is associated with charge transfer between unoccupied metal and ligand sites. In the limit $|\Delta| \gg |t|$, all charge transfer processes between ligands and metals lead only to virtual occupation of the latter.

2.3. PERTURBATION THEORY

In the above scenario, the fluctuations of the orbital occupation are small. They can be treated in perturbation theory in the coupling and provide a transparent understanding of the system. We derive an effective model by eliminating the charge degrees of freedom on the metal sites and represent their effect as an effective tunnel coupling between the ligands. An example of a virtual process giving rise to this coupling is shown in Figure 4. Technically, we project out single occupied metal states using second-order Brillouin–Wigner perturbation theory (equivalent to a Schrieffer–Wolff transformation [12]). The resulting effective model (up to a constant) takes the form of the well-known extended Hubbard model on the four ligand sites:

$$H_{\text{eff}} = -\sum_{\langle jk\rangle} \sum_{\sigma} T a^{\dagger}_{j,\sigma} a_{k,\sigma} + H_L, \tag{5}$$

describing the low-energy properties of the mobile electrons on the [2 × 2]-grid. Here $T = (t^2/2\Delta) \ll t$, Δ is the effective hopping amplitude.

3. Results

We now analyze the effective Hamiltonian derived by perturbation theory in Eq. (5) for the reduction steps with n = 0–8 additional electrons on the system. In the noninteracting limit of the effective model (u = 0), we find a low-lying MO at energy $\epsilon - 2T$, two degenerate MOs at ϵ (due to the 4-fold symmetry axis), and one at $\epsilon + 2T$. Filling these levels according to the Pauli principle, the ground-state spin for odd particle number n is S = 1/2. For even n = 2, 6, the ground state has S = 0,

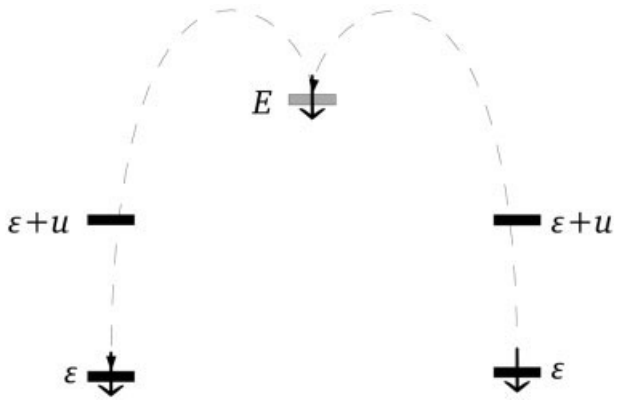

FIGURE 4. Energy diagram showing an example of a charge transfer from one ligand to another ligand by virtual occupation of a Fe^{2+}-ion state in the middle.

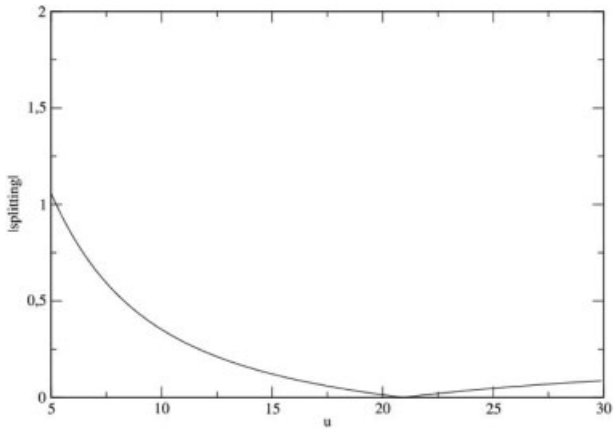

FIGURE 5. Fe^{2+}-[2 × 2] grid showing excitation gap as a function of u for $n = 3$ extra electrons for $T = 1$, $v = 2$, $w = 0.5$. For $u \approx u_{cr} \approx 21T$, the splitting is zero: the Nagaoka state and the nonferromagnetic state (quartet or doublet) are degenerate. For $u > u_{cr}$, the Nagaoka state is the ground state.

whereas for half-filling ($n = 4$), $S = 0$ and $S = 1$ are degenerate. In the presence of interaction $u \neq 0$, the triplet contribution for $n = 4$ is suppressed and we have singlet ground state. For $u \gg T$, charge fluctuations are suppressed, and we have a Heisenberg antiferromagnet; i.e., electron spins on neighboring ligands couple antiferromagnetically.

For sufficiently large $u > u_{cr} \approx 21T$ (Fig. 5), the ground-state spin for odd $n = 3, 5$ is enhanced from the noninteracting value $S = 1/2$ to the maximal possible value $S = 3/2$ (Fig. 6). Relative to the half-filled state $n = 4$ a hole/electron can gain kinetic energy when moving in a fully polarized background of the other electrons. This ferromagnetic alignment competes with the antiferromagnetic spin coupling due to superexchange processes. The underlying mechanism for the spin ordering was first described in the context of the Nagaoka theorem [13], which guarantees that the ground state has maximal spin if $u > u_{cr}$. The theorem applies to the effective model (5) because the model fulfills the connectivity condition that an "exchange loop" no longer than four sites exists [14, 15]. By moving a hole along such an "exchange" loop, it is possible to access every spin configuration for fixed total S_z. Then all basis states with common S_z are connected with each other via nonvanishing matrix elements of Eq. (5). Tasaki defined in his paper a loop of length m by an ordered set of sites $(s_1, \ldots, s_m)$ such that $t_{s_i s_{i+1}} \neq 0$ for all $i = 1, \ldots, m - 1$, and $t_{s_m s_1} \neq 0$. If the loop is longer than four sites, it is possible to find two configurations with common S_z that cannot be connected via hopping matrix elements because spins with different projection cannot be exchanged in the subspace of forbidden double occupancy. For this reason, the Nagaoka theorem does not apply to a model with eight equivalent sites.

Whether superexchange or kinetic energy gain dominate depends on the relative strength u/T of the onsite repulsion. We find a critical value of $u_{cr}/T \approx 21$ (Fig. 5). Considering the fact that T arises from a weak hybridization of near-orthogonal orbitals, the Nagaoka limit of the system may be reached. Chemical modification of the ligands that draw charge density in the ligand LUMOs toward the center of the ligand, thereby reducing T, will tend to enhance the effect. The density-dependent interactions v, w merely increase the critical value u_{cr} for the Nagaoka state but do not destroy it [16]. The gap separating the maximal spin ground state from excitations rises to $0.05T$ at $u \approx 25T$ and saturates slowly with increasing $(u - u_{cr})$ around approximately $0.23T$.

The addition spectrum can be understood in terms of the effective electrostatic interactions in the effective model 5. The first electron reduces one of the four ligands. The next one occupies the opposite ligand in order to minimize the Coulomb interaction. The third and fourth electrons reduce the adjacent ligands. For the next four electrons, this sequence of processes is repeated. As a result, we predict two sets of four reduction peaks separated by a gap of order u, each set consisting of two pairs of peaks separated by $v \ll u$ (see Fig. 7 for $T/t \ll$

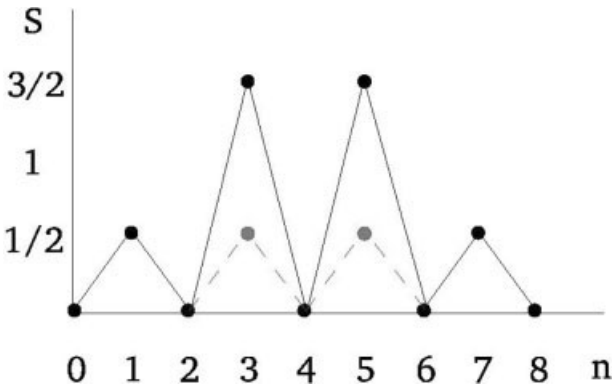

FIGURE 6. Fe^{2+}-[2 × 2] grid showing ground-state spin as function of the number of electrons added to the ligands for $T = 1$, $u > u_{cr} \approx 21$ (black line) and $u < u_{cr}$ (red line).

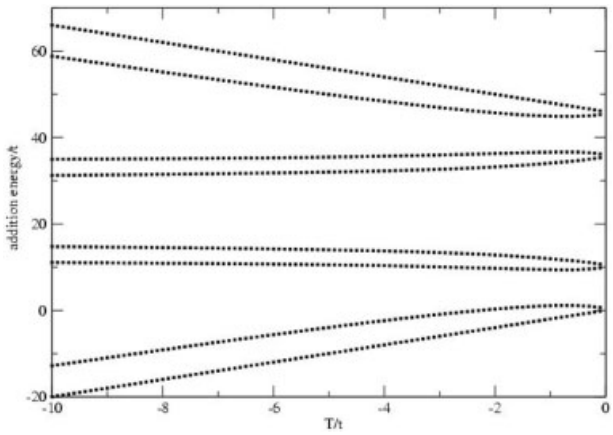

FIGURE 7. Fe^{2+}-[2 × 2] grid showing addition energy determined from the full model 1 as function of tunneling amplitude $T = t^2/(2\Delta)$ for fixed other parameters $u = 25$, $v = 5$, $w = 0.5$. For $T/t \ll 1$, we are in the perturbative regime, where no spin is localized on the Fe^{2+} site.

1). This is in agreement with the experimental observations [9]. The perturbation theory applies in the regime $T/t \ll 1$. As an independent check, we have calculated the positions of the reduction peaks using the full Hamiltonian 1 by exact diagonalization for any T/t. These are shown in Figure 7.

4. Conclusions

We have developed and analyzed a phenomenological model for [2 × 2]-grid complexes with Fe^{2+} transition-metal centers to explain the cyclic voltammogram and to elucidate the interplay between electron addition and intramolecular spin coupling. Our model contains both localized magnetic moments and itinerant electrons, in contrast to the customary description of molecular magnets. We have found that the model reproduces the experimental addition energy spectra [9] for the iron complex.

The total spin as a function of number of added electrons for small to moderate charging energies (u/T) oscillates between $S = 0$ and $S = 1/2$ due to antiferromagnetic coupling between spins on the ligands via the bridging metals. In a tunneling transport experiment, the localized spin 1/2 on the molecule for odd n should give rise to a Kondo spin-screening effect, whereas transport is Coulomb blocked for even n.

However, for sufficiently large u/T, we predict a change in the magnetic coupling between the additional electrons, which can lead to the occurrence of a maximal total spin state near half-filling of the four ligand orbitals ($n = 3, 5$). Here the Nagaoka mechanism is at work: due to the Pauli principle, a missing or excess electron can be delocalized fully when the "background" of the remaining electrons is completely spin-polarized. We note that both parameters can be tuned chemically by modification of the ligands. In this scenario, the total spin changes by more than one-half between subsequent ground states of the molecule. Single electron tunneling experiments through the complex with a gate voltage tuned near half-filling of the ligand orbitals will reveal the large change in ground-state spin as a spin blockade of tunneling [17, 18]. We expect the spin selection rules to suppress the single-electron tunneling around transitions $2 \to 3$, $3 \to 4$, $4 \to 5$, and $5 \to 6$ and the Kondo effect for $n = 3, 5$. Experimental detection of sublattice and total magnetization as a function of the number of added electrons would also be of great interest.

Finally, we note that the electrochemical experiments [9] are performed near room temperature where thermal occupation of high-spin excited states of the individual metal-ions becomes possible [19, 20]. A generalization of our model to include the high-spin states of the ions is highly nontrivial but also of great interest. The high-spin states are metastable and the spin-crossover physics must be incorporated in sufficient detail to yield a reasonable starting model (e.g., vibronic coupling of the ground-state and excited state nuclear potential sheets, higher excited states). While clearly outside the scope of the present study, the results obtained are a useful starting point for the analysis of such finite temperature behavior of the system.

ACKNOWLEDGMENTS

The authors thank the Deutsche Forschungsgemeinschaft for financial support within the SPP 1137 Molekularer Magnetismus, Project SCHO 641/3-1. M. R. W. acknowledges the financial support provided through the European Community's Research Training Networks Programme under contract HPRN-CT-2002-00302, Spintronics.

References

1. Sessoli, R.; Tsai, H.-L.; Schake, A.; Wang, S.; Vincent, J.; Folting, K.; Gaschetti, D.; Christou, G.; Hendirckson, D. J Am Chem Soc 1993, 115, 1804.
2. Aubin, S.; Sun, Z.; Pardi, L.; Krzystek, J.; Folting, K.; Brunel, L.-C.; Rheingold, A.; Cristou, G.; Hendrickson, D. N. Inorg Chem 1999, 38, 5329.
3. Friedman, J. R.; Sarachick, M.; Tejada, J.; Ziolo, R. Phys Rev Lett 1996, 76, 3830.
4. Wernsdorfer, W.; Sessoli, R. Science 1999, 284, 133.
5. Barbara, B. J Magn Magn Mater 1999, 200, 167.
6. Leuenberger, M. N.; Loss, D. Nature 2001, 410, 789.
7. Hanan, G. S.; Schubert, D. V. U. S.; Lehn, J. M.; Baum, G.; Fenske, D. Angew Chem Int Ed Engl 1997, 36, 1842.
8. Zhao, L.; Matthews, C. J.; Thomson, L. K.; Heath, S. L. Chem Commun 2000, 4, 265.
9. Ruben, M.; Breuning, E.; Barboui, M.; Gisselbrecht, J. M.; Lehn, J. M. Chem Eur J 2003, 1, 9.
10. Semenow, A.; Spatz, J. P.; Möller, M.; Lehn, J. M.; Sell, B.; Schubert, D.; Weidl, C. H.; Schubert, U. S. Angew Chem 1999, 111, 2701.
11. Semenow, A.; Spatz, J. P.; Möller, M.; Lehn, J. M.; Sell, B.; Schubert, D.; Schubert, C. H. W. U. S. Angew Chem Int Ed 1999, 38, 2547.
12. Schrieffer, J. R.; Wolff, P. A. Phys Rev 1966, 149, 491.
13. Nagaoka, Y. Phys Rev 1966, 147, 392.
14. Tasaki, H. Phys Rev B 1989, 40, 9192.
15. Tasaki, H. Prog Theor Phys 1998, 99, 489.
16. Kollar, M.; Strack, R.; Vollhardt, D. Phys Rev B 1996, 53, 9225.
17. Weinmann, D.; Häusler, W.; Kramer, B. Phys Rev Lett 1995, 74, 984.
18. Ono, K.; Tarucha, S. cond-mat/0309062 (2003).
19. Breuning, E.; Ruben, M.; Lehn, J. M.; Renz, F.; Garcia, Y.; Ksenofontov, V.; Gütlich, P.; Wegelius, E.; Rissanen, K. Angew Chem Int Ed 2000, 14, 39.
20. Ruben, M.; Breuning, E.; Lehn, J. M.; Ksenofontov, V.; Renz, F.; Gütlich, P.; Vaughan, G. B. M. Chem Eur J 2003, 9, 4422.